Physicochem. Probl. Miner. Process., 56(5), 2020, 797-817

http://www.journalssystem.com/ppmp

Physicochemical Problems of Mineral Processing

ISSN 1643-1049

Received January 13, 2020; reviewed; accepted July 22, 2020

Acidified water glass in the selective flotation of scheelite from calcite, part II: species in solution and related mechanism of the depressant

Nathalie Kupka [1], Peter Kaden [2], Anne Jantschke [3], Edgar Schach [1], Martin Rudolph [1]

[1] Helmholtz Institute Freiberg for Resource Technology, Helmholtz-Zentrum Dresden-Rossendorf, Chemnitzer Straße 40, 09599 Freiberg, Germany

[2] Institute of Resource Ecology, Helmholtz-Zentrum Dresden-Rossendorf, Bautzner Landstraße 400, 01328 Dresden, Germany

[3] Bioanalytical Chemistry, TU Dresden, Bergstraße 66, 01609 Dresden, Germany

Corresponding author: n.kupka@hzdr.de, sternath@gmail.com (Nathalie Kupka)

Abstract: Sodium silicate is one of the main depressants against calcite and fluorite in the scheelite flotation industry. In the first part of this article, the authors acidified sodium silicate (AWG) with three acids (sulfuric, oxalic and hydrochloric) to improve its performance. Results showed that acidified water glass outperforms alkaline water glass in terms of selectivity: it increases mainly the grade by further depressing silicates and calcium-bearing minerals. In most cases, AWG requires lower dosages to do so. The effect of acidified water glass is evaluated through Mineral Liberation Analysis (MLA), froth analysis, Raman and Nuclear Magnetic Resonance (NMR) spectroscopy in order to hypothesize its mechanism. MLA shows that AWG affects silicates and sulfides more intensely than semi-soluble salt-type minerals. Froth observations indicate other species in solution associated to the acid having an impact on the flotation results. Raman spectroscopy and NMR measurements indicate that the solution undergoes deep depolymerization when water glass is acidified. Lower molecular weight silica species, specifically Si-O monomers such as $SiO(OH)_3^-$ will be responsible for the depression of the gangue minerals and are the drivers of the selectivity of AWG, more than orthosilicic acid. Depolymerization is more or less effective depending on the mass ratio of the acid to water glass and depending on the acid.

Keywords: acidified water glass, scheelite calcite separation, froth flotation, mechanism

1. Introduction

Sodium silicate is one of the main depressants for calcite, fluorite and silicates in the scheelite flotation industry. In the first part of this article, based on literature, we acidified sodium silicate with three acids (sulfuric, oxalic and hydrochloric) to improve its performance. Indeed, acidified water glass (AWG) is supposed to have a stronger depressing effect on gangue at lower dosages than alkaline water glass (Fuerstenau et al., 1968; Yang et al., 2016).

Part I showed that acidified water glass outperforms alkaline water glass in terms of selectivity (Kupka et al., 2020a): it increases mainly the grade by further depressing silicates and calcium-bearing minerals. In most cases, it requires lower dosages to do so. The type of acid is not relevant as all three acids show an increased selectivity but best results were obtained for oxalic acid and hydrochloric acid in the investigated system. The dosage of acid and its mass ratio to sodium silicate are crucial parameters for the preparation of acidified water glass with the greatest impact on flotation.

In this second part of our article, the behavior of acidified water glass (AWG) is investigated in order to determine which species in solution are responsible for its higher performance and where is the depressant truly impactful, either in the pulp or in the froth or both. Its effect is evaluated through Mineral Liberation Analysis (MLA), froth analysis, Raman and Nuclear Magnetic Resonance (NMR) spectroscopy. For the first time, a review of relevant silica chemistry and adsorption studies together

DOI: 10.37190/ppmp/125639

with an analysis of the silica species in solution taking into account other potential species allow the building of a comprehensive hypothesis for the mechanism of acidified water glass.

2. Material and methods

Based on the results presented in the first part of this article, seven of the batch flotation tests are selected for this investigation: WG_500 as a point of comparison to sodium silicate, SA51_500, SA51_350, OA51_500, OA51_350, HCl31_350 and HCl31_500 as the best performing tests for each acid. The protocols of the selected tests are found in Table 1.

Table 1. Protocols of the tests selected for this article

Test number	pH	Regulators (g/t)		Acid (g/t)		Collector (g/t)	Frother (g/t)
		Sodium carbonate	Sodium silicate	Ratio Acid: Water glass	Hydrochloric acid	Sodium oleate	Flotanol 7197
WG_500	9	100	500				
SA51_350	9	100	350	1:5	70	200	20
SA51_500	9	100	500	1:5	100	200	20
OA51_350	9	100	350	1:5	70	200	20
OA51_500	9	100	500	1:5	100	200	20
HCl31_350	9	100	350	1:3	117	200	20
HCl31_500	9	100	500	1:3	167	200	20

2.1. Preparation of acidified water glass

Acidified water glass was produced using analytical grade of sodium metasilicate nonahydrate ($Na_2O_3Si.9H_2O$) with a modulus of 1:1 from Aldrich Chemistry mixed with three different acids: sulfuric acid (H_2SO_4), oxalic acid ($C_2H_2O_4$) and hydrochloric acid (HCl) from Carl Roth. Sodium silicate comes as a powder. It is prepared as a solution of 4.76 % (w/w) which is the dissolution limit of this specific powder. Additionally, a sodium silicate solution is most stable in concentrations in the range of 2 % to 5 % according to Bulatovic (2007). The oxalic acid solution was prepared at the same mass concentration while hydrochloric acid and sulphuric acid were prepared at 1 mol/l. Sodium silicate is mixed with the acid and stirred on a magnetic stirrer for 30 min at ambient lab temperature (21°C). The solutions of AWG were always directly transferred to the flotation cell without any downtime to increase the reproducibility and the comparability of the tests.

2.2. Froth analysis

The ore used for batch flotation tests contains 0.51 % scheelite, 1.70 % calcite, 0.28 % apatite by mass and various silicates (quartz, micas, plagioclases and hornblende). Details of the flotation protocol can be found in Part I (Kupka et al., 2020a). The three points on the diagrams are the cumulative concentrates taken a t = (1, 3, 7) min. During each batch flotation test, pictures of the side of the transparent flotation cell are taken at 2 s intervals with a MoticCam camera with 3Mpx resolution. The pictures are then processed with ImageJ® in order to extract the froth and the bubble information as described in Schach et al. (2017). Statistical analyses of the data are conducted with RStudio®.

2.3. Mineral Liberation Analysis (MLA)

Representative sample powders were prepared as A-side grain mounts (Heinig et al., 2015) and carbon coated with a Leica EM MED 020. MLA is a FEI Quanta 650F scanning electron microscope equipped with two Bruker Quantax X-Flash 5030 EDX detectors and ThermoFisher/FEI's MLA Suite 3.1.4 for automated data acquisition (Fandrich et al., 2007). XBSE measurements were conducted at the Helmholtz Institute Freiberg at an accelerating voltage of 25 kV and a probe current of 10 nA. The data were processed using the programming language R following the methodology presented in Kupka et al. (2020b).

The minerals of the ore have been regrouped into representative groups to simplify the processing of automated mineralogy data and based on common flotation properties (Table 2). This grouping was established based on the results from Kupka et al. (2020b).

Table 2. Mineralogical composition of the ore (the main mineral constituting the group is underlined)

Groups	Minerals	Average feed in % (w/w)
Phyllosilicates	Biotite, muscovite, serpentine	7.86
Quartz		15.20
Scheelite		0.51
Semi-soluble salt-type minerals	Ankerite, apatite, calcite, fluorite	1.99
Silicates	Augite, cummingtonite, hornblende, epidote, orthoclase, plagioclase, titanite	73.03
Sulfides	Arsenopyrite, bismuthinite, chalcopyrite, molybdenite, pentlandite, pyrite, pyrrhotite, sphalerite	1.34
Trace	Hematite, ilmenite, rutile, zircon	0.05

The flotation rate constant k for scheelite was calculated based on the classical first order kinetics equation (Sutherland, 1948). It was plotted using a gaussian kernel density estimate, whose description and methodology can be found in Schach et al. (2019) and Hoang et al. (2019).

2.4. Raman spectroscopy

Raman spectra were collected with a DXR SmartRaman (Thermo Fisher Sientific Inc.) with 532 nm laser excitation operating at a power of 10 mW and using a 1800 gr/mm grating and a 25 μm aperture resulting in a 1.6 cm^{-1} to 2 cm^{-1} spectral resolution. The spectral range was 40 cm^{-1} to 1800 cm^{-1} and the exposure time was 5 s with 50 accumulations (measurement time around 4 min). Measurements were taken every five minutes over a total reaction time of 30 min. All spectra were baseline corrected and were therefore limited to a range of 40 to 1550 cm^{-1}.

2.5. Nuclear Magnetic Resonance

NMR spectra were measured with an Agilent DD2-600 NMR spectrometer equipped with an Agilent One probe operating at 599.80 MHz and 119.16 MHz for Proton and Silicium-29, respectively. Spectra were collected with standard Agilent pulse programs. The samples were prepared in 5 mm quartz tubes with a coaxial insert containing toluene-d6 for frequency locking and shimming and TMS as internal standard. Sample solutions were measured directly after preparation. Silicium-29 spectra were averaged over 8192 scans with a recovery delay of 10 s resulting in 24 h of measuring time. All spectra were processed with 10 Hz line broadening, were background corrected for amorphous silica species of probe parts and line fitted and the resulting spectra are subsequently evaluated.

3. Interaction of acidified water glass with different mineral groups

Five of the batch flotation tests were selected for Mineral Liberation Analysis: WG_500, SA51_500, OA51_350, OA51_500 and HCl31_500. The cumulative recovery of scheelite presented in Fig. 1a proves that the presence of acidified water glass does in general favour the flotation of scheelite. Fig. 1b shows that AWG improves the selectivity of the flotation, even though the process in general remains unselective when it comes to semi-soluble salt-type minerals. The tests with oxalic acid show that the dosage of the acid might be crucial to its impact on semi-soluble salt-type minerals, a potential explanation for which is given in 5.7.

Regarding other gangue minerals, such as the sulfides and the silicates, acidifying the water glass greatly improves selectivity as compared to alkaline water glass (Fig. 2). AWG affects silicates and sulfides more intensely than semi-soluble salt-type minerals. Higher selectivity is achieved with hydrochloric and sulfuric acid.

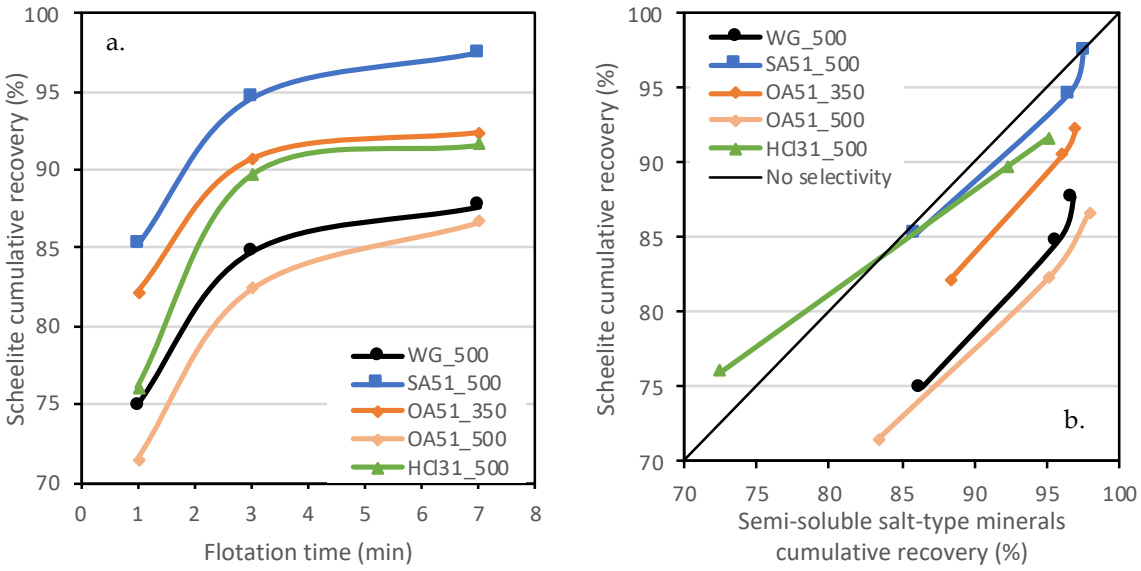

Fig. 1. Scheelite recovery a) depending on the flotation time and b) against the recovery of the semi-soluble salt-type minerals (at flotation times 1, 3 and 7 min)

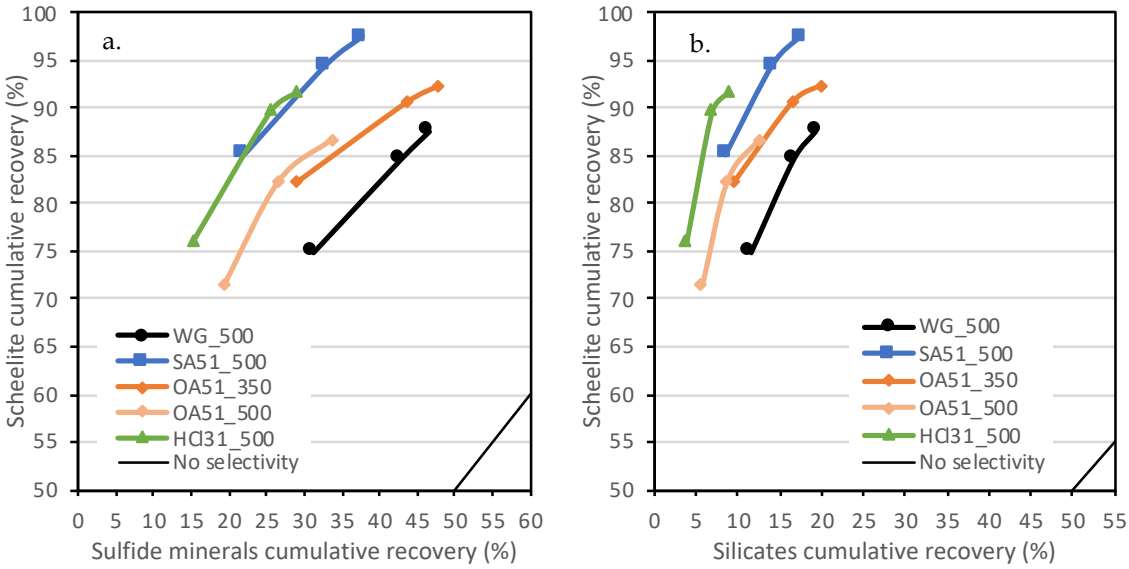

Fig. 2. Scheelite recovery against a) the sulfide recovery and b) silicates recovery (at flotation times 1, 3 and 7min)

In the feed, ~97.7% of the scheelite surface is more than 80% liberated. Therefore, surface liberation does not play a major role in this specific flotation system. However, Fig. 3 shows a contrasted image when using kernel density estimates and calculating the expected flotation rate constant of scheelite depending on its size and its degree of surface liberation. Coarser more liberated scheelite particles float faster while the distribution of the scheelite particles displays a lot of fines, which would point at some overgrinding before the flotation tests. Fig. 3d and Fig. 3e indicates a faster flotation of the scheelite fines with a higher dosage of the depressant. By depressing other minerals and thus inducing higher amounts of available collector, AWG allows middlings and locked particles of scheelite to be collected at a faster rate, especially for hydrochloric acid and sulfuric acid. Said particles do not float as fast in the case of oxalic acid. In general, hydrochloric acid slows down the flotation of scheelite while sulfuric acid accelerates it and oxalic acid is somewhere in between.

An entrainment factor EF for a mineral of size class i can be calculated for the gangue minerals based on the equation of Yianatos and Contreras (2010), which is the ratio of R_G the recovery of the free gangue particles and R_w the water recovery. For entrainment calculations, particles considered liberated have over 95 % f ree surface. Fig. 4 and Fig. 5 display the entrainment of quartz, phyllosilicates and silicates

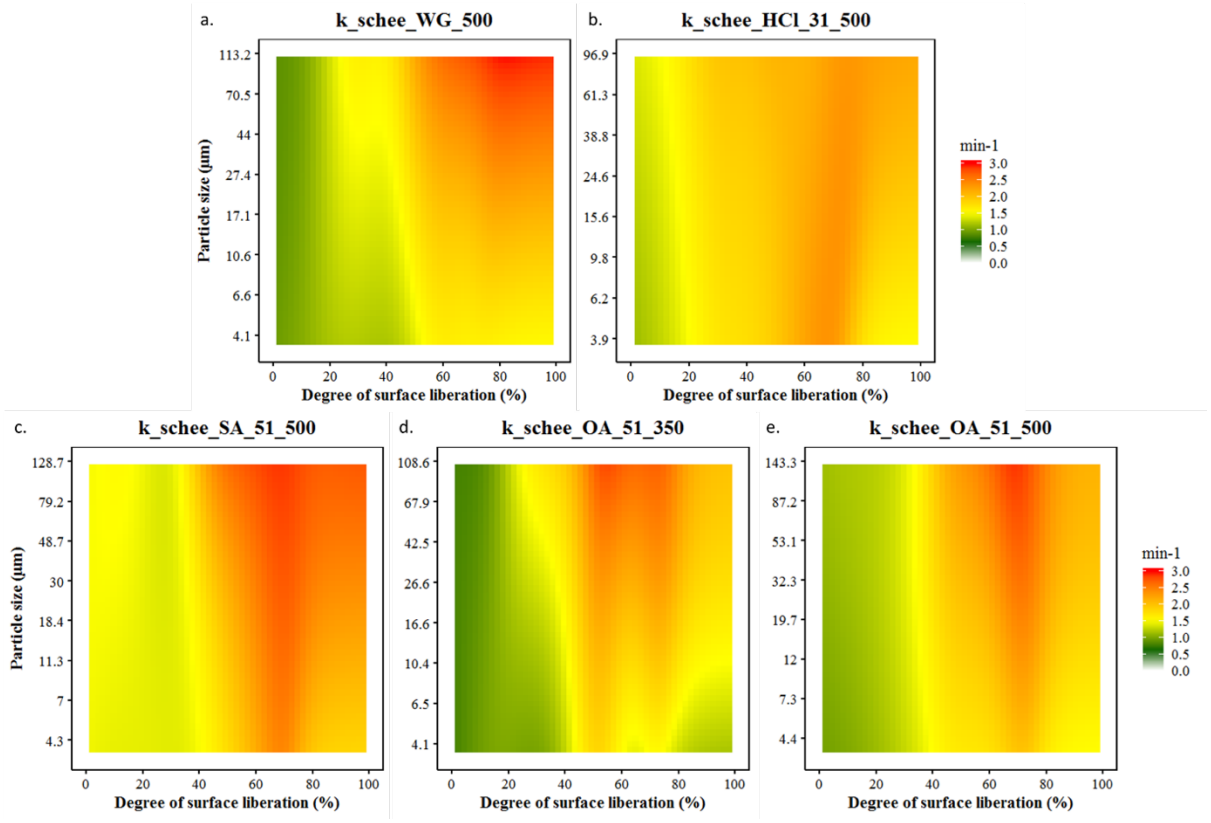

Fig. 3. Flotation rate constant of scheelite *k* depending on its degree of surface liberation and its size (calculated as the log of the equivalent circle diameter and converted back to µm for the diagrams)

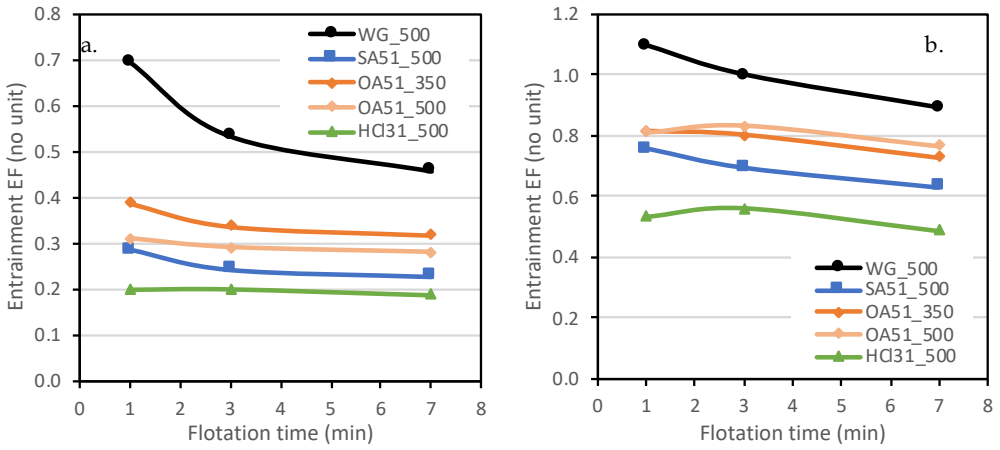

Fig. 4. Entrainment of a) quartz and b) phyllosilicates

(sulfide entrainment was not calculated as sulfides are receptive to fatty acid collectors). The comparatively high entrainment of other silicates can be explained by a small part of true flotation of the calcium-bearing silicates, which has been observed in other works (Foucaud et al., 2019a; Kupka et al., 2020b). Entrainment of silicates in general is reduced, with AWG-SA and AWG-HCl having a larger impact than AWG-OA. True flotation of silicates is lowered but a reduction of true entrainment would be linked to froth characteristics being affected.

4. Influence of acidified water glass on froth characteristics

Flotation performance is heavily affected by phenomena in the froth zone and thus the froth characteristics, which impacts both the mineral and the water recoveries and therefore entrainment (Hoang et al., (Hoang et al., 2018; Neethling and Brito-Parada, 2018). Fig. 6presents the 30 s median froth and for better comparison Fig. 7 the corresponding 60 s normalized averages.

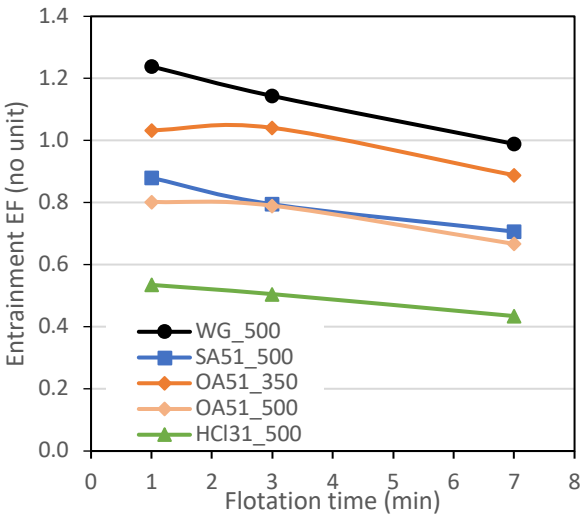

Fig. 5. Entrainment of other silicates

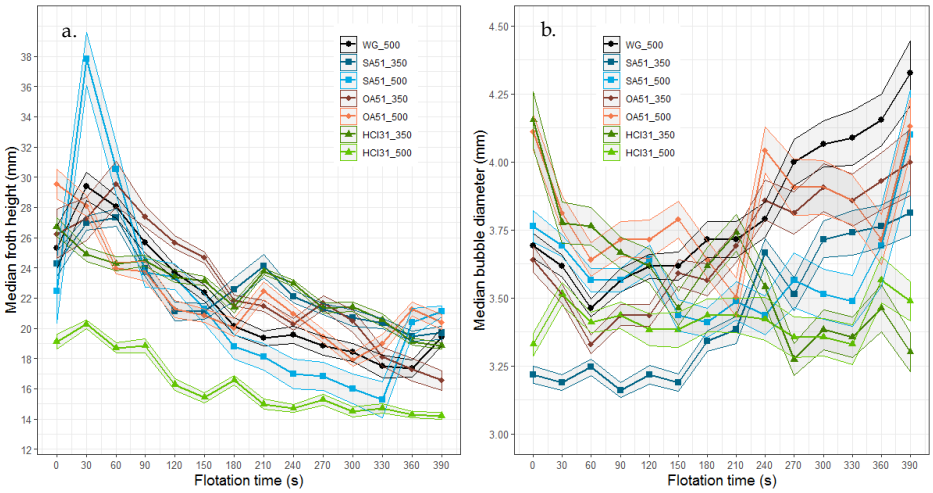

Fig. 6. 30 s median a) froth height and b) bubble diameter in the froth (the ribbons are the 95% confidence interval)

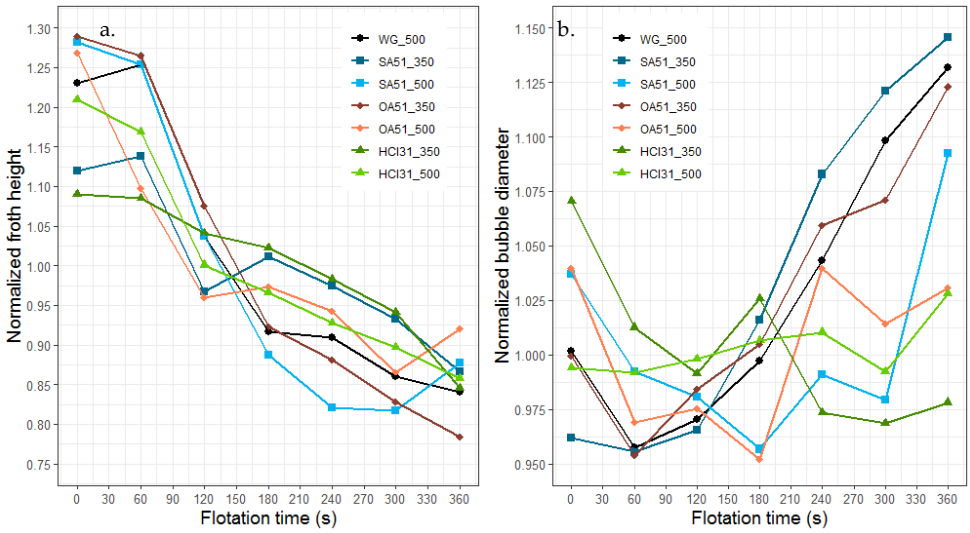

Fig. 7. 60 s average a) froth height and b) bubble diameter in the froth normalized to their respective averages

In terms of froth height, the tendency is the same for all the tests: as expected, they all decrease with flotation time. SA51_500 and OA51_350 have almost an identical evolution to WG_500, OA51_500 and

HCl31_500 are very similar to it while HCl31_350 and SA51_350 are similar only to each other as their decrease is not as intense and is flatter in comparison with the other tests. Looking at the normalized bubble diameters, the results are different: only three tests display the expect trend of bubble coarsening of flotation time, WG_500, SA51_350 and OA51_350, to the point that they are almost identical. SA51_500 and OA51_500 are similar in that the bubble diameter decreases over time before increasing at the same point in time. Hydrochloric tests display a much flatter trend, whereby the bubble diameter for HCl31_350 slightly decreases.

Fig. 8 presents the average bubble diameter at the bottom half of the froth and the corresponding ratio of the top to bottom diameters as a proxy for bubble coalescence. The first is an indirect estimation of the bubble size in the pulp. On one hand, as these are batch flotation tests, it is expected that the bubble size in the pulp would increase steadily with the decreasing frother concentration over flotation time. This can be observed for SA51_350 and OA51_350 which are identical to WG_500. All other tests however display a different trend: SA51_500 and OA51_500 show a much more chaotic but less intense increase in the bottom bubble diameter while hydrochloric tests are either flat or decreasing. On the other hand, tests with AWG usually display a higher bubble coalescence than the other tests, the highest being HCl31_500 where clearly a very high dosage of hydrochloric acid has an important impact on the bubble size. SA51_350 is also relatively flat but follows WG_500's trend as does OA51_350. HCl31_350 is the only test that shows a clear increase in bubble coalescence over time.

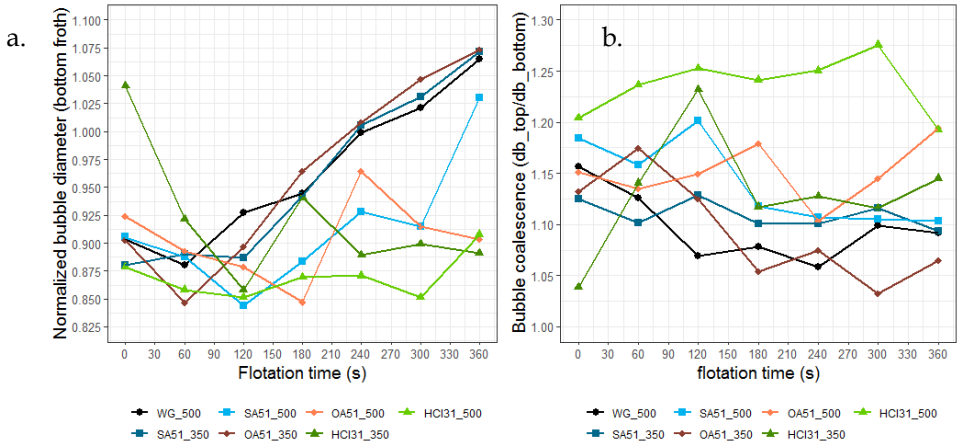

Fig. 8. a) 60 s average of the bubbles normalized to their average in the bottom half of the froth and b) Bubble coalescence against flotation time as the ratio of the bubble diameter of the top half of the froth divided by the bubble diameter of the bottom half of the froth normalized to their averages

Overall, the impact of acidified water glass might not appear directly on the froth height but definitely affects bubble sizes. SA51_350 and OA51_350 display almost identical trends to WG_500 and are also the tests that performed closest to alkaline water glass in terms of tungsten grade and recovery (see Part I). As a consequence, adding a little bit of oxalic or sulfuric acid to sodium silicate induces the necessary amount of required species in solution to have the same impact on the bubble size, amongst others. A higher dosage of these acids lead to a smaller bubble size in the pulp and a higher bubble coalescence than with simple water glass. Finally, the addition of hydrochloric acid already in a small quantity induces a smaller bubble size in the pulp over time, which could mean that the progressive depletion of hydrochloric acid in the pulp is associated to a destabilisation of the film of the bubbles. A higher dosage of hydrochloric acid has a drastic result: the bubble size in the pulp is among the smallest and is the most stable of all tests, inducing a very high bubble coalescence over time. An explanation for these differences is provided in 5.7.

5. Mechanism of acidified water glass

5.1. Polymerization of silica

To understand the mechanism behind the effects of acidified water glass, it is necessary to identify the type of silica species forming in solution, their level of polymerization and their amount. Indeed, silica species are supposed to be responsible for the depression of the gangue minerals.

Silica species in solution are noted Q^n depending on their degree of polymerization, whereby Q is the silicon atom and n (from 0 to 4) is the number of bridging oxygen atoms (Vidal et al., 2016). Polymerization is understood here in its broader sense and can be defined as a "*mutual condensation of Si(OH) to give molecularly coherent units of increasing size*" (Iler, 1979). Structures of the Q species are summarized in Table 3 (Sjöberg, 1996).

Table 3. Structure of silica species depending on the polymerization degree

Notation	Structure
Q^0	Monomeric silicates
Q^1	Dimeric silicates and end chain groups
Q^2	Middle groups in chains or cycles
Q^3	Chain branching sites
Q^4	Three-dimensionally crossed linked groups

Polymerization of silica cannot occur without orthosilicic acid ($Si(OH)_4$, Q^0 species). Equations 1 to 7 describe said polymerization at different pH values (compiled from Balinski (2019), Belton et al. (2012), Iler (1979), Zuhl and Amjad (2013) and Weres et al. (1980)).

$$2Si(OH)_4 \rightleftharpoons Si(OH)_3^+ + SiO(OH)_3^- + H_2O \quad (1)$$

$$Si(OH)_3^+ + SiO(OH)_3^- \rightleftharpoons Si_2O(OH)_6 \quad (2)$$

Below pH 2, changes are expected to take hours:

$$Si(OH)_4 + H^+ \rightleftharpoons Si(OH)_3^+ + H_2O \quad (3)$$

$$Si(OH)_3^+ + Si(OH)_4 \rightleftharpoons Si_2O(OH)_6 + H^+ \quad (4)$$

Above pH 2, changes are faster:

$$Si(OH)_4 + OH^- \rightleftharpoons SiO(OH)_3O^- + H_2O \quad (5)$$

$$SiO(OH)_3^- + Si(OH)_4 \rightleftharpoons Si_2O(OH)_6 + OH^- \quad (6)$$

At all pH:

$$Si_2O(OH)_6 + Si(OH)_4 \rightleftharpoons Si_3O_2(OH)_8 + H_2O \quad (7)$$

Further polymerization will involve the Q^3 species formed to condense into ring structures which turn into larger molecules by addition of monomers, so into oligomers which condense into particles. Above pH 7, these changes are instant and take seconds or minutes. The degree of polymerization of sodium silicate is dependent on its modulus, e.g. the SiO_2 to Na_2O ratio. As a consequence, the higher the ratio, the higher the polymerization (Mishra, 1982). The sodium metasilicate nonahydrate used in this study has a ratio of 1:1 and is expected to yield a relatively low amount of polymerized species.

When put in solution, alkaline water glass produces silicic acid $Si(OH)_4$ at pH below 9.4, $SiO(OH)_3^-$ above pH 9.4 and $SiO_2(OH)_2^{2-}$ above pH 12.6 (Deng et al., 2019; Feng et al., 2015; Tian et al., 2019). Martins and Amarante (2012) and Wilhelm and Kind (2015) state that adding sulfuric acid yields the following reaction:

$$Na_2SiO_3 + H_2O + H_2SO_4 \rightleftharpoons Si(OH)_4 + Na_2SO_4 \quad (8)$$

We would generalize the reaction for all acids as follows:

$$Na_2SiO_3 + H_3O^+ + H^+ \rightleftharpoons Si(OH)_4 + 2Na^+ \quad (9)$$

As a consequence, adding acid should saturate the solution with orthosilicic acid and therefore increase its polymerizing ability. This is probably why Berlinskii and Klyueva (1972) and Yongxin and Changgen (1983) claim that AWG has higher polymerizing ability than alkaline water glass. It is necessary to identify if highly polymerized silica species or low molecular weight silica species are responsible for the depression of the minerals and how these species vary depending on the acid type, amongst other parameters.

5.2. Rate of polymerization

The rate of polymerization is indicated by the amount of time required to build up a gel. A description of the appearance of different solutions of acidified water glass at different mass ratios can be found in

Table 4 with photographic examples in Fig. 9 It indicates how important the mass ratio of the acid to sodium silicate can be: for example, all three types of acidified water glass build up a gel over time but at very different mass ratios and at different speeds. Oxalic acid is the only acid leading to the build-up of crystals and its gel tends to be heterogeneous while the gel of hydrochloric and sulfuric acid is homogeneous. The crystals are in insufficient number to be analyzed so there is no certainty that they are silica-related. The rate of polymerization is extremely fast for sulfuric acid (less than an hour), moderately paced for oxalic acid (a few hours) and very slow for hydrochloric acid (weeks).

Table 4. Description of the solutions of acidified water glass at different mass ratios at a constant temperature of 21°C (coloration means a color change from transparent to creamy white)

Acid	Mass ratio	1h	3h	6h	24h	1 week	4 weeks	10 weeks
Hydrochloric acid	1:1							
	3:1							
	4:5						Coloration	Gelling
	4.75:1						Coloration	Gelling
	5:1					Particles		
	5.25:1							Particles
	5.5:1							Particles
Oxalic acid	1:1						Crystals	
	2.5:1					Coloration	Gelling	
	2.75:1					Coloration	Gelling	
	3:1			Coloration	Gelling			
	3.25:1		Coloration	Gelling				
	3.5:1						Coloration	Gelling
	5:1							Particles
Sulfuric acid	1:1							
	2.5:1							
	2.75:1							Gelling
	3:1	Coloration	Gelling					
	3.25:1					Gelling		
	3.5:1							Particles
	5:1							Particles

5.3. Solution pH

The sodium silicate concentration in solution as well as its pH value determines the type of complexes formed in solution prior to their adsorption onto mineral surfaces (Yang et al., 2008). The pH of acidified water glass depends on the mass ratio of sodium silicate to the acid and the acid type. Therefore, the pH of the solutions at mass ratios of water glass to acid of 1:1, 3:1 and 5:1 was measured at different time intervals (Fig. 10) to determine if there are any observable reactions and how fast they would stabilize. The pH is stable for most solutions, indicating that outside of silica polymerization or depolymerisation (which is pH neutral), there are no side reactions. Sulfuric acid at 3:1 is an exception, where the origin of the increase in pH is unclear.

Orthosilicic acid condensates at different rates depending on the pH of the solution as mentioned before (Fig. 11). Based on Table 4, Fig. 10 and Fig. 11, acidified water glass at a mass ratio of 5:1 should produce a stable sol whereas at 3:1 and 1:1 aggregation can be observed. The reaction is catalyzed differently depending on the acid: for hydrochloric acid, H^+ is the main catalyzer while for sulfuric and oxalic acids, OH^- is the main catalyzer. The rate of condensation is also different for the three acids, with oxalic and sulfuric acid leading to the highest rates while condensation through hydrochloric acid will remain low, which corresponds well to the previous observations.

The pathways to silica formation from orthosilicic acid to sols or gels depends on the pH and the presence of salts as presented in Fig. 12 and in concordance with Table 4. Indeed, solutions at a mass ratio of 5:1 have a high pH, a low concentration of salts since there is little acid and result in a sol. This sol turns into a suspension after several weeks due to the generation of large particles. Solutions at a

mass ratio of 1:1 and 3:1 have a low pH and lead to the build up of a gel. Only sulfuric acid at 3:1 would, from a pH point of view, be expected to end up in a sol, but the high concentration of sulphate anions possibly affects the solution to the point of building the gel anyways.

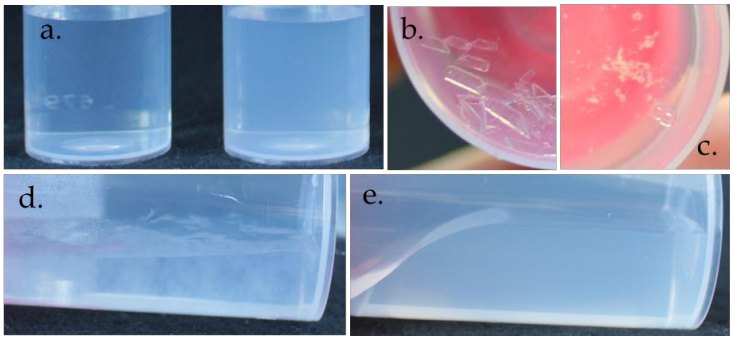

Fig. 9. Different solution appearances: a. transparent and cloudy solutions, b. crystals, c. particles, d. heterogeneous gel, e. homogeneous gel

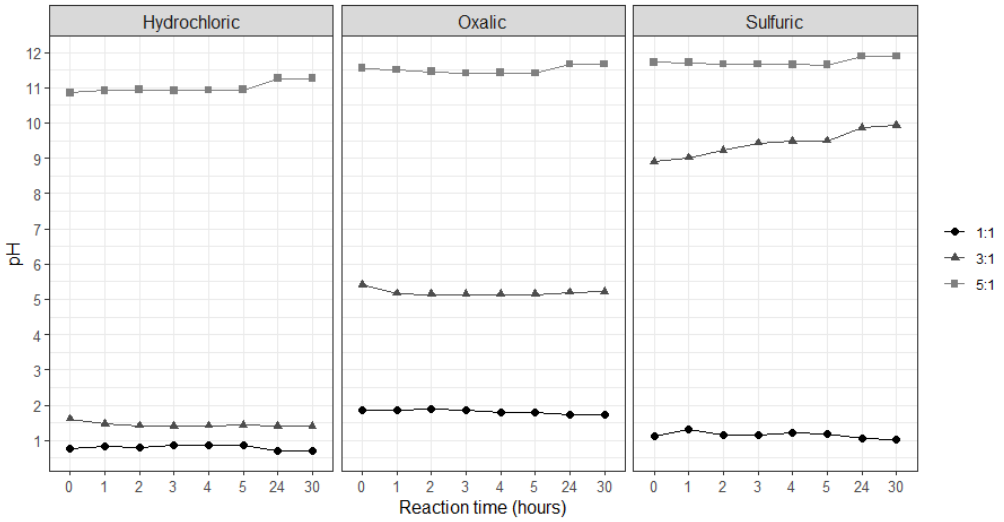

Fig. 10. Evolution of pH depending on the reaction time between sodium silicate and the acid

5.4. Degree of polymerization

NMR measurements were conducted on solutions of acidified water glass at a mass ratio of 5:1 in order to determine the degree of polymerization of the solution depending on the acid type (and thus on the solution pH). 5:1 is the mass ratio at which oxalic and sulfuric acid perform best and it was maintained

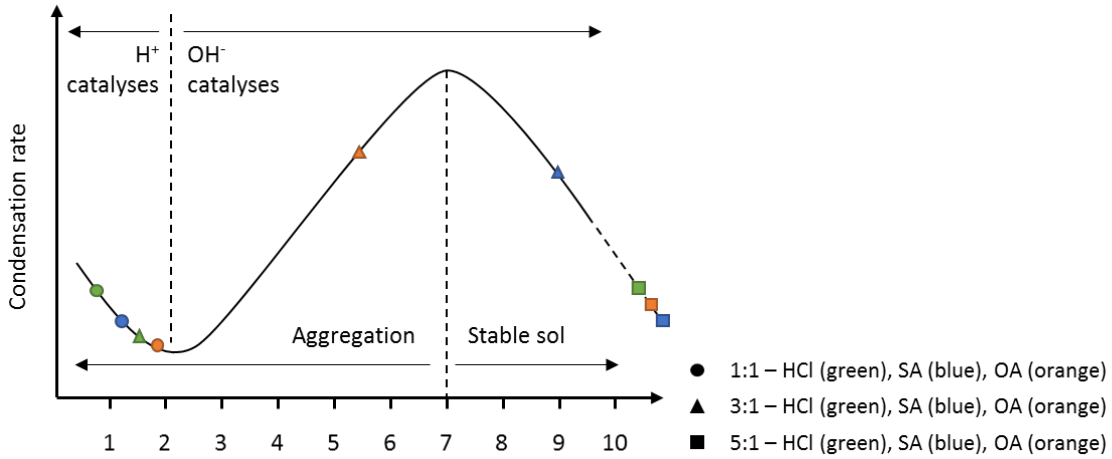

Fig. 11. Condensation rate of silicic acid depending on pH (Cordes, 2006; Spinde, 2012) with the pH measured for the different AWG (HCl = Hydrochloric acid, SA = Sulfuric acid, OA = Oxalic acid) at different mass ratios

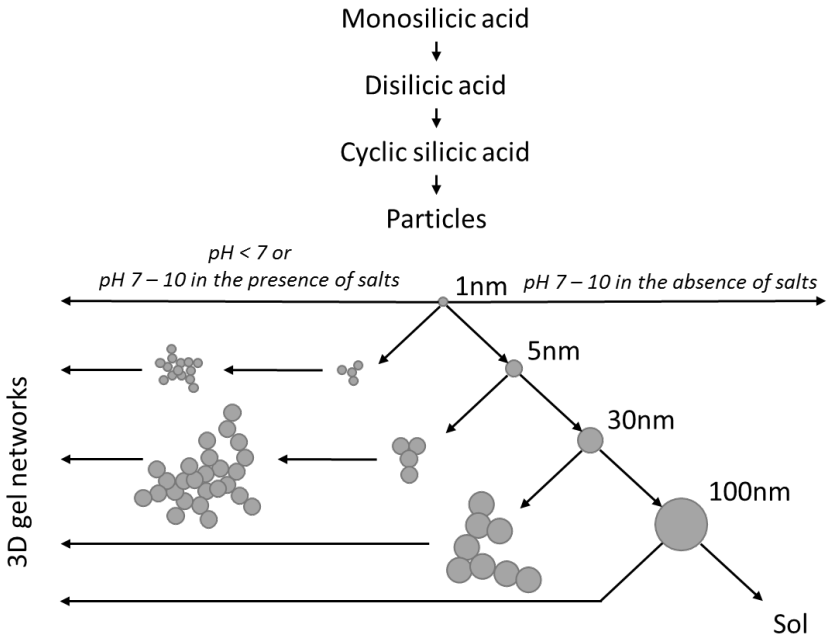

Fig. 12. Pathways to silica formation from orthosilicic acid to sols or gels depending on the pH and the salt concentration (modified from Iler (1979))

at 5:1 for hydrochloric as well for comparison purposes. The degree of polymerization of silicic acid can be assessed through its chemical shift (Table 5).

The processed NMR spectra are found in Fig. 13. All three acids generate Q^0 to Q^3 species, but Q^3 species are only quantifiable with oxalic acid. The peak area ratios normalized to the Q^0 peak are listed in Table 6. The grade of polymerization is comparable for sulfuric and oxalic acid, with a similar production of Q^1 and Q^2 species, with a minor preference of oxalic acid to generate trimeric structures. Hydrochloric acid, however, yields a high amount of trimeric species with a higher amount of Q^2, e.g. it tends to polymerize more or at least faster than the other acids at this mass ratio. This leads to the hypothesis that adding acid in the water glass solution prevents polymerization or leads to depolymerisation depending on the mass ratio of the acid to sodium silicate, e.g. the pH of the solution. Moreover, the fact that these measurements represent the average spectra of the 3 solutions over 24 hours proves that even with a long stirring time of the solution, only low molecular weight species are expected.

Table 5. Ranges of the chemical shift of ^{29}Si at different degrees of polymerization (compiled by Spinde (2012))

Structure	Notation	Chemical shift (ppm)
Monomer	Q^0	-70.0 to -72.0
Dimer	Q^1	-77.5 to -80.7
Cyclic trimer	Q^2_{tri}	-80.0 to -82.3
Trimer	Q^2	-88.0 to -90.5
Branched oligomer	Q^3	-92.6 to -98.2
Network oligomer	Q^4	-108.0 to -110.0

Table 6. Peak area ratios normalized to the Q^0 peak (level of polymerization of the species increasing from left to right)

Acid	Q^0	Q^1	Q^2_{tri}	Q^2	Q^3
Sulfuric	1	0.56	0.12	0.80	
Oxalic	1	0.60	0.24	0.73	0.42
Hydrochloric	1	0.64	0.62	0.93	

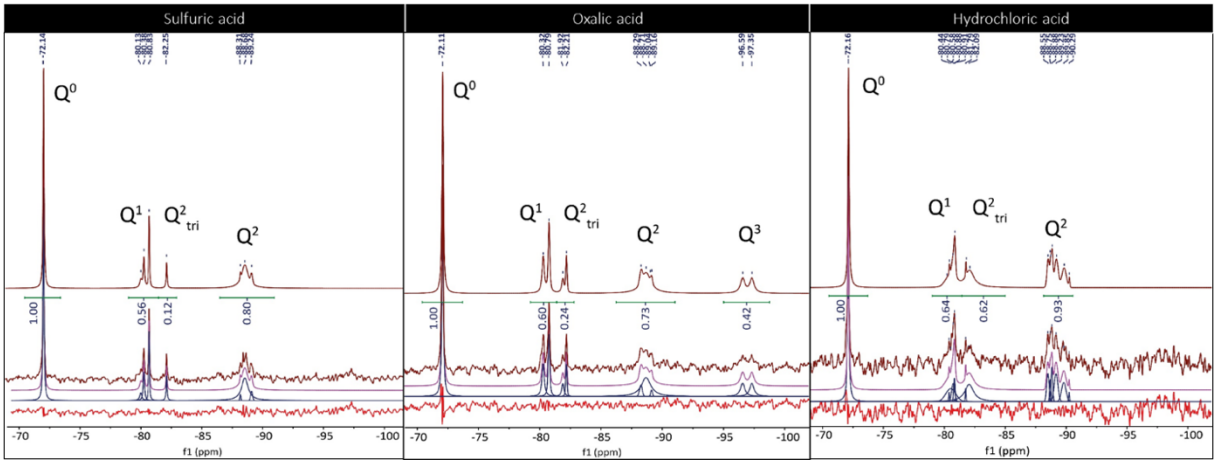

Fig. 13. ^{29}Si NMR spectra of 5:1 acidified water glass solutions with from top to bottom: Fitted spectrum with peak positions and integrals of the respective Q^n domains, original spectrum (dark red), sum of fitted peaks (pink), fitted peaks (blue), residual of fitting (red)

5.5. Identification of the species

Based on Fig. 10, Fig. 11 and the NMR results, it is possible that the type of acid is irrelevant but that the solution pH resulting from the mixing of sodium silicate with the acid is the most crucial parameter for the subsequent flotation. Therefore, it is necessary to look at the species in solution to identify possible differences linked to the acid type and to determine if a lower degree of polymerization is indeed the advantage of AWG over WG.

To identify the species present in solution, Raman spectra of solutions at mass ratios of water glass to acid of 1:1, 3:1 and 5:1 were measured every 5 min for 30 min (the reaction time used for batch flotation tests) and compared to the Raman spectra of the individual reagents. The averaged spectra can be found in Annex 1. Silicate species bands were identified based on the studies from Vidal et al. (2016) and Halasz et al. (2007), sulfuric acid species bands were assigned based on Cox et al. (1981) and oxalic acid species based on Saksena (1940). In general, silica species do not scatter well and are therefore not easily detected by Raman spectroscopy. All Raman spectra were collected under identical conditions and allow qualitative comparison.

First, from the acid type point of view, pure oxalic acid related bands show that the C-C stretching vibration at 844 cm^{-1} disappears in solutions of 3:1 and 5:1 and is partially gone and/or shifted at 1:1. Carboxylic acid is most likely completely dissociated in the 3:1 and 5:1 solutions and consumed by a reaction (condensation and/or depolymerisation). For sulfuric acid, HSO_4^- related bands at 595, 896, 1053 and 1210 cm^{-1} disappear completely in 3:1 and 5:1 solutions while the SO_4^{2-} band at 981 cm^{-1} increases intensely, showing that the proton is indeed consumed by a reaction.

Second, in the case of silica species, Q^0 species are identifiable for all acids, while Q^1 species can only be assigned for oxalic acid, Q^2 species for hydrochloric acid, Q^3 and Q^4 species for all three acids. The corresponding band assignments for the silica species are presented in Table 7.

Table 7. Silica species band assignments depending on the solutions

Band	Assignment	Water glass	Hydrochloric acid			Oxalic acid			Sulfuric acid		
			1:1	3:1	5:1	1:1	3:1	5:1	1:1	3:1	5:1
633.0	Q^0 : Si-O monomers	X	X	X	X	X	X	X		X	X
777.5	Q^0: SiO_4^{4-}	X	X	X	X	X	X	X	X	X	X
900.0	Q^1	X					X	X			
920.0	Q^2	X	X	X							
1025.8	Q^3	X			X		X	X			
1068.2	Q^3	X			X		X	X			X
1115.0	Q^3/Q^4	X								X	X

The average Raman intensity for each species is presented in Fig. 14. The intensity values have been recalculated based on the water glass concentration to take into account that each solution had a different silica concentration at t = 0 min. This allows directly comparing the band intensities of the mixtures with pure water glass.

Q^0 species are produced in higher or equivalent amounts to water glass, especially for oxalic and hydrochloric acid. 3:1 tests with sulfuric acid and oxalic acid display a lot less orthosilicic acid. This is expected from the condensation rate shown in figure 11 because these two solutions have pH values closer to pH 7 and therefore a higher condensation rate compared to the other samples. These two tests also underperformed in froth flotation. Q^1 species are only observable with oxalic acid and at higher mass ratios, but in much higher amounts than in pure water glass. Q^2 species are observed with hydrochloric acid at lower mass ratios in equivalent amounts to pure water glass. Q^3 species are best observable with oxalic acid, which was expected from the NMR measurements. Sulfuric acid is the only acid that clearly leads to the formation of Q^3 / Q^4 species.

Fig. 15 shows the evolution of the band intensity ratio of the Q^0 silica species in the mixtures to the Q^0 silica species in pure water glass based on the reaction time. The production of Q^0 species is relatively stable in 3:1 and 5:1 solutions, which correlates well with the NMR measurements and also indicates that the reaction reaches its equilibrium almost instantly. In 1:1 solutions, said production decreases more or less intensely depending on the acid, indicating a slower reaction. The ratio could not be calculated for sulfuric acid at 1:1 mass ratio due to an overlapping band of sulfuric acid related bands hiding the Q^0 band.

As a reminder, flotation tests with sulfuric and oxalic acid at a mass ratio of 5:1 performed better than the mass ratio of 3:1. 5:1 and 3:1 sulfuric acid mixtures lead to a higher production of Si-O monomers. 5:1 oxalic acid mixtures lead to a higher production of all Q^0 species while 3:1 only showed Si-O monomers. In the case of hydrochloric acid, the tests at 3:1 performed better than 5:1. Both 3:1 and 5:1 mixtures lead to a higher production of Si-O monomers but not of orthosilicic acid.

Overall, the Raman observations corroborate the NMR measurements and confirm that mixing sodium silicate with an acid leads to a higher production of low molecular weight species. They also

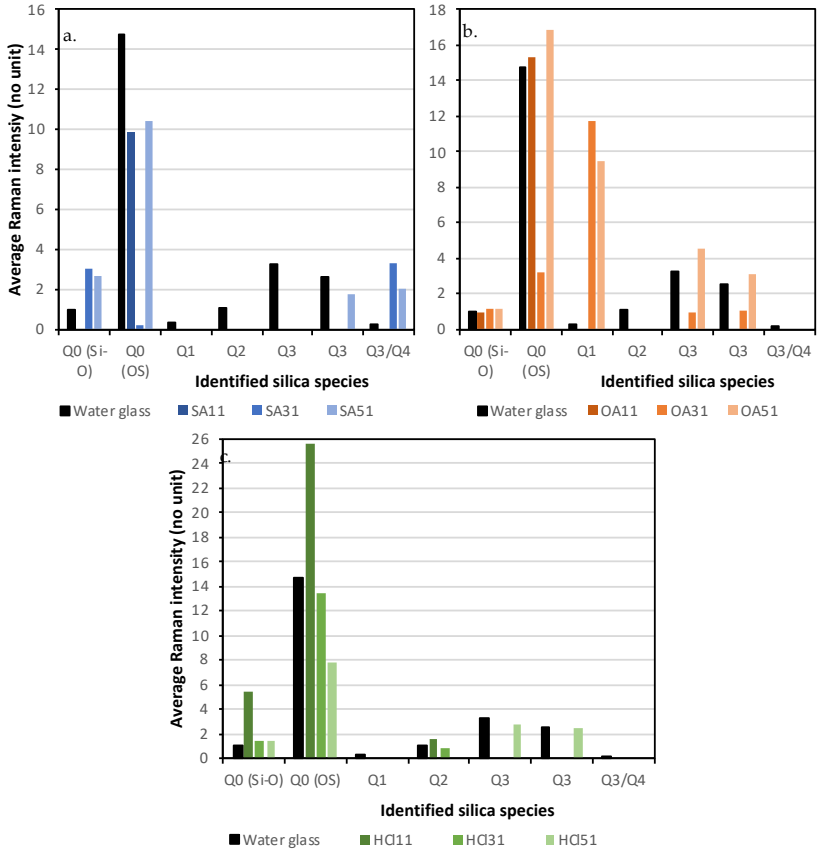

Fig. 14. Average Raman band intensity of the silica species for all the mass ratios recalculated based on the water glass concentration (OS = orthosilicic acid) for a) sulfuric acid, b) oxalic acid and c) hydrochloric acid

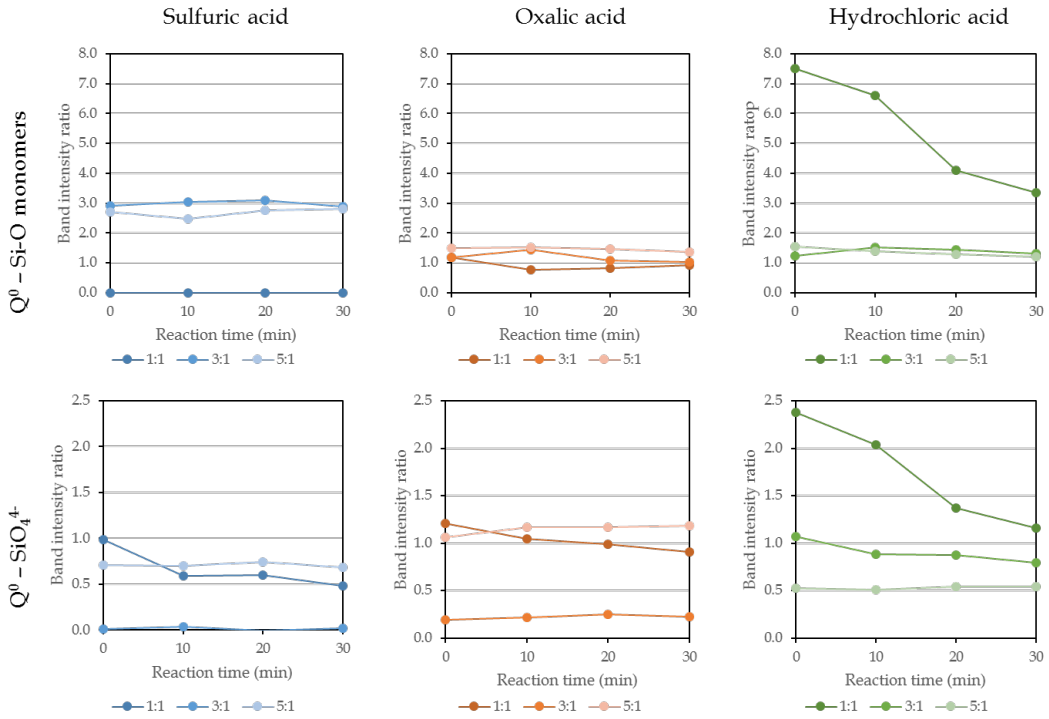

Fig. 15. Evolution of the Raman band intensity ratio of the Q^0 silica species in the mixtures to the Q^0 silica species in pure water glass over the reaction time

correlate well with the pH of the solutions and the related literature: a pH between 4 and 10 corresponds to a high condensation rate of orthosilicic acid while a pH outside these ranges leads to depolymerisa tion of the water glass solution. Iler (1979) and Zhou and Lu (1992) had already asserted this hypothesis. The depolymerisation and the high production of lower molecular weight silica species is actually beneficial to flotation. On a side note, 1:1 hydrochloric acid mixtures have a high performance potential based on the high production of Q^0 species but the solution would need to be used right away as the reaction is very unstable.

Overall, the Raman observations corroborate the NMR measurements and confirm that mixing sodium silicate with an acid leads to a higher production of low molecular weight species. They also correlate well with the pH of the solutions and the related literature: a pH between 4 and 10 corresponds to a high condensation rate of orthosilicic acid while a pH outside these ranges leads to depolymerisa tion of the water glass solution. Iler (1979) and Zhou and Lu (1992) had already asserted this hypothesis. The depolymerisation and the high production of lower molecular weight silica species is actually beneficial to flotation. On a side note, 1:1 hydrochloric acid mixtures have a high performance potential based on the high production of Q^0 species but the solution would need to be used right away as the reaction is very unstable

5.6. Hypothesis on the mechanism

In literature, water glass is assumed to precipitate on the surface of calcium minerals as nearly insoluble calcium silicate through $SiO(OH)_3^-$ (Marinakis and Shergold, 1985) or through colloidal silica (Fuerstenau et al., 1968; Martins and Amarante, 2012), preventing collector adsorption. Colloidal silica consists normally in colloidal silicon dioxide and is so used in our article but the aforementioned authors do not state what species they define as “colloidal silica”.

Many authors that worked with acidified water glass have used different techniques to demonstrate a greater absorption of AWG on the gangue mineral than on the valuable mineral (Table 8). In general, they showed that the zeta potential of the gangue mineral (mostly calcite) would become more negative while the zeta potential of the valuable mineral would remain relatively constant. In this study, MLA data confirm the direct interaction of AWG with minerals.

According to Dong et al. (2018), the selectivity of AWG is due to the fact that calcite is positively charged while scheelite is negatively charged. They identify the species adsorbing onto calcite as

Table 8. Method use to show greater adsorption of AWG on the gangue mineral than on the valuable mineral

Authors	Method			
	Zeta potential	IR	FTIR	Adsorption test
Deng et al. (2019)	X			
Zhou and Lu (1992)		X		
Tian et al. (2019)	X			
Liu et al. (2016)	X			
Feng et al. (2015)	X		X	
Dong et al. (2018)	X			
Yang et al. (2016)	X			X

$SiO_2(OH)_2^{2-}$ and $SiO(OH)_3^-$ through X-ray photoelectron spectrometry studies, which is also the assumption of Martins and Amarante (2012), Marinakis and Shergold (1985) and of Deng et al. (2019). Feng et al. (2015) considered $Si(OH)_4$ to be the central species. Azizi and Larachi (2018), in a study on alkaline sodium silicate, showed that $SiO(OH)_3^-$ interacts more strongly with calcium-mineral surfaces than $Si(OH)_4$ due to covalent bonding as opposed to hydrogen bonding. Complementary to this, Foucaud et al. (2019b) demonstrated that the more polymerized dimer $Si_2O(OH)_6$ physisorbs onto fluorite but at a lower rate than the less polymerized forms. Marinakis and Shergold (1985) suggest the following surface reactions:

$$Ca^{2+}_{surface} + SiO(OH)^{3-} \rightleftharpoons Ca^{2+}\text{-}SiO(OH)_{3\,(surface)} \quad (10)$$

$$CaOH^{2+}_{surface} + Si(OH)_4 \rightleftharpoons Ca^{2+}\text{-}OSiO(OH)_{3\,(surface)} + H_2O \quad (11)$$

Based on the Raman spectroscopy results and NMR measurements and confirming literature observations, it seems that by acidifying water glass e.g. adding a large amount of hydrogen cations, the solution undergoes deep depolymerization, removing the highly condensed species. Zhou and Lu (1992) suggested that silica depolymerisation yields low molecular weight silicate species such as $H_5SiO_4^+$, $Si(OH)_4$, $SiO(OH)_3^-$, $Si_2O(OH)_6H^+$, $Si_2O(OH)_6$ or $Si_2O_2(OH)_5^-$. We suggest the reactions would be written as follows:

$$Si_3O_2(OH)_8 + H_3O^+ \rightleftharpoons Si_2O(OH)_6 + Si(OH)_4 + H^+ \quad (12)$$

$$Si_2O(OH)_6 + H_3O^+ \rightleftharpoons 2Si(OH)_4 + H^+ \quad (13)$$

$$SiO_2(OH)_2^{2-} + H_3O^+ \rightleftharpoons SiO(OH)_3^- + H_2O \quad (14)$$

$$SiO(OH)_3^- + H_3O^+ \rightleftharpoons Si(OH)_4 + H_2O \quad (15)$$

Based on the Raman observations, we consider that Si-O monomers such as $SiO(OH)_3^-$ are the lower molecular weight species responsible for the depression of the gangue minerals as they interact more strongly with the mineral surfaces than more polymerized species. This depolymerization will be more or less effective depending on the mass ratio of the acid to water glass and depending on the acid, in other words, depending on the induced pH: a too large pH value does not lead to this depolymerization and prevents acidified water glass to perform as well as alkaline water glass. Ideally, the pH of the solution would need to be lower than 4 or higher than 10.

Within the semi-soluble salt-type mineral group, their higher depression as compared to scheelite would be linked to a higher affinity of the low molecular weight silica species to calcite and fluorite. This is likely linked to the higher calcium surface site density and higher calcium surface activity of these minerals (summarized in Kupka and Rudolph (2018)). Sodium silicate however has a very high affinity to silicate minerals (Foucaud et al., 2019a) so it is not surprising that AWG is a better depressant for silicates than for semi-soluble salt-type minerals.

5.7. Other species involved

The addition of acid in large quantities does not only generate species required for the depolymerization of alkaline sodium silicate, it also generates ions not silica-related which could have a separate impact on flotation.

First, sodium carbonate is used in all the flotation tests presented in this study. The presence of sodium carbonate has been demonstrated to enhance the depressing action of alkaline sodium silicate on semi-soluble salt-type minerals through its carbonate ion CO_3^{2-} (Foucaud et al., 2019a) by a combination of calcium surface site density, calcium activity and surface carbonation (Kupka and Rudolph, 2018). Additionally, silicates may be activated by calcium ions in the pulp, which sodium carbonate prevents through pulp and surface precipitation while also hindering their activation through its cation Na^+ (Martins and Amarante, 2012). This synergy is also expected to happen with acidified water glass.

At pH values higher than 2.5 sulfuric acid is dissociated as SO_4^{2-} and H^+ ions while at pH lower than 1 it is partially dissociated as HSO_4^- and H^+ (Casas et al., 2000). Atademir et al. (1980) investigated the use of sodium dodecyl sulfate (SDS) as a collector in scheelite flotation and demonstrated that SO_3^- adsorbs onto scheelite at minority positive sites but displays a much higher adsorption onto calcite. They however showed that these differences did not generate any contrast in the flotation of the mixed minerals and that SDS could not be considered a collector in this case. Several studies involve mixing sodium silicate with Fe(II) or Al sulfates to improve flotation (Deng et al., 2018; Foucaud et al., 2019a; Patil and Nayak, 1985; Tian et al., 2019). If the metallic cation does impact flotation, the sulfate anion is not discussed. As a consequence, even though this anion certainly interacts with other species in solution or may adsorb onto mineral surfaces, its impact on minerals can be considered either negligible or nonexistent.

It is less simple in the case of oxalic acid. Oxalic acid has a known affinity to calcium-bearing minerals and was demonstrated to depress titanaugite via chemisorption onto its surface by reaction with calcium ions to form insoluble metal carboxylate complexes (Liu et al., 2015). It was also tested as a depressant in scheelite flotation by Yin et al. (2015) where its impact was more limited. In general, oxalic acid is the simplest dicarboxylic acid. In solution, it exists as an oxalate anion ($C_2O_4^{2-}$) at pH above 4, as $HC_2O_4^-$ at pH values between 1 and 4 and below 1 as $H_2C_2O_4$. The oxalate anion contains two carboxylate anions (COO^-), which are known to bond their two oxygen atoms with two neighboring calcium atoms on mineral surfaces, making them the main collecting mechanism of fatty acids, including sodium oleate (Foucaud et al., 2018; Rao and Forssberg, 1991). Its impact could therefore be either positive, e.g. it helps collect scheelite, or negative, e.g. it lowers the selectivity by collecting other semi-soluble salt-type minerals. Results presented in Fig. 1 would suggest that both can happen: if the dosage of oxalic acid is too high, it lowers process selectivity but if well dosed, oxalic acid helps collect scheelite.

Finally, a relationship between solution ionic strength and the bubble Sauter mean diameter in the pulp has been derived by many authors, with the higher the ionic strength the smaller the diameter (Michaux et al., 2018) even though high salt concentrations are required to significantly affect bubble coalescence in the pulp (Castro et al., 2013). Craig (2004) established a combining rule of ion pairs that inhibit coalescence in the pulp, whereby ions are classified as α or β and only pairs of the same class have an impact on coalescence. Ion pairs relevant to this study are presented in Table 9.

The water associated with the flotation tests related to this study was not analyzed however, the presence of Na^+, K^+, Mg^{2+} and Ca^{2+} in the water is guaranteed. Ca^{2+} is most likely the cation in the highest concentrations. In 4, the impact of acidified water glass on the froth is described and shows that hydrochloric tests had the most visible effect on froth-related parameters. Based on Craig (2004), chlorine anions have many possibilities to combine with cations in the water to reduce bubble coalescence and are the only ones to pair with Ca^{2+}, the main cation. Hydrochloric tests were indeed the ones involving the lowest inferred bubble diameter in the pulp and a very high dosage of hydrochloric acid resulted in an unchanging bubble diameter over time. Based on these results, hydrochloric acid is most likely heavily reducing bubble coalescence in the pulp. This would also explain why entrainment is so limited (Fig. 4 and Fig. 5) and partially why the grade is so high but the recovery lower with HCl31_500, as smaller bubbles have a smaller wake and a lower loading potential. This is the only expected additional impact of chlorine.

In the case of sulfuric and oxalic acid, the effect is not as recognizable, even though high dosages of these acids (e.g. OA51_500 and SA51_500) did show smaller bubbles sizes in the pulp than their lower dosages or WG_500. This is likely to be because they have less potential pairs. In terms of froth-related parameters, anions of the three acids might have other effects that cannot be identified without a dedicated systematic study, which is not the purpose of this article.

Table 9. Relevant ion pairs with an impact on bubble coalescence (Craig, 2004), a check indicates that the combination does inhibit coalescence, a cross no effect observed and an empty cell refers to non-tested pairs or to pairs that are not sufficiently soluble to reach the required concentration to affect coalescence

	Cations	H^+	Na^+	K^+	Mg^{2+}	Ca^{2+}
Anions	Type	β	α	α	α	α
OH^-	α	✗	✓	✓		
Cl^-	α	✗	✓	✓	✓	✓
SO_4^{2-}	α	✗	✓		✓	
$(COO)_2^{2-}$	α	✗		✓		

6. Conclusions

In this article, a hypothesis on the mechanism of acidified water glass is proposed. The impact of AWG was studied through Mineral Liberation Analysis (MLA) and froth analysis of rougher lab flotation tests as well as Raman and Nuclear Magnetic Resonance spectroscopy.

Based on MLA analyses, it becomes clear that acidified water glass can indeed depress semi-soluble salt-type minerals and to a larger extent, sulfides and silicates. It also affects the entrainment of gangue minerals by partially affecting the bubble coalescence in the pulp: with a higher dosage of acid, the bubbles in the pulp tend to be smaller and bubble coalescence in the froth is higher than with alkaline sodium silicate. Hydrochloric acid has the highest impact on the bubble coalescence in the pulp compared to oxalic and sulfuric acid, where it is more limited. A small part of the performance of acidified water glass is linked to its impact on the pulp bubbles itself.

Silicic acid $Si(OH)_4$ is the main silica species produced by alkaline water glass in solution at pH below 9.4, above pH 9.4, it is $SiO(OH)_3^-$ and above pH 12.6 $SiO_2(OH)_2^{2-}$. These species polymerize at different rates depending on the solution. The rate of polymerization is extremely fast for sulfuric acid, moderately paced for oxalic acid and very slow for hydrochloric acid. The reaction is catalyzed differently depending on the acid: for hydrochloric acid, H^+ is the main catalyzer while for sulfuric and oxalic acids, OH^- is the main catalyzer.

Based on the Raman spectroscopy results and NMR measurements, the solution undergoes deep depolymerization when water glass is acidified. It can be expected that lower molecular weight species, specifically Si-O monomers such as $SiO(OH)_3^-$ will be responsible for the depression of the gangue minerals and are the drivers of the selectivity of AWG, more than orthosilicic acid. This depolymerization will be more or less effective depending on the induced pH of the solution, which is determined by the mass ratio of the acid to water glass and depending on the acid. From that point of view, the type of acid could be considered irrelevant whilst the pH of the mixture should be lower than 4 or higher than 10.

However, studying the other species generated in solution by the addition of acids leads to the assumption that using just any type of acid with sodium silicate is not optimal. On one hand, oxalic acid could be more recommended than other acids even though its use is delicate: too high a dosage lowers process selectivity but if well dosed, oxalic acid helps collect scheelite, increasing recovery. On the other hand, the correct dosing of hydrochloric acid can prevent bubble coalescence in the pulp, reducing entrainment and increasing grade but limiting recovery. In the end, the choice of the acid is like every other challenge in flotation: it is a question of compromise and priorities.

Acknowledgments

The authors thank Arsenii Rybalchenko for conducting the pH measurements and Kristine Trinks for the MLA measurements.

Annex 1: Raman spectra

Raman spectra of the pure reagents (WG = water glass, SA = sulfuric acid, , OA = oxalic acid, HCl = hydrochloric acid) as compared to the Raman spectra of the mixtures (11 = mass ratio of 1:1 of water glass:acid, 31 = mass ratio of 3:1, 51 = mass ratio of 3:1). The concentration of the pure reagents is higher and therefore yields higher peak intensities than for the mixtures.

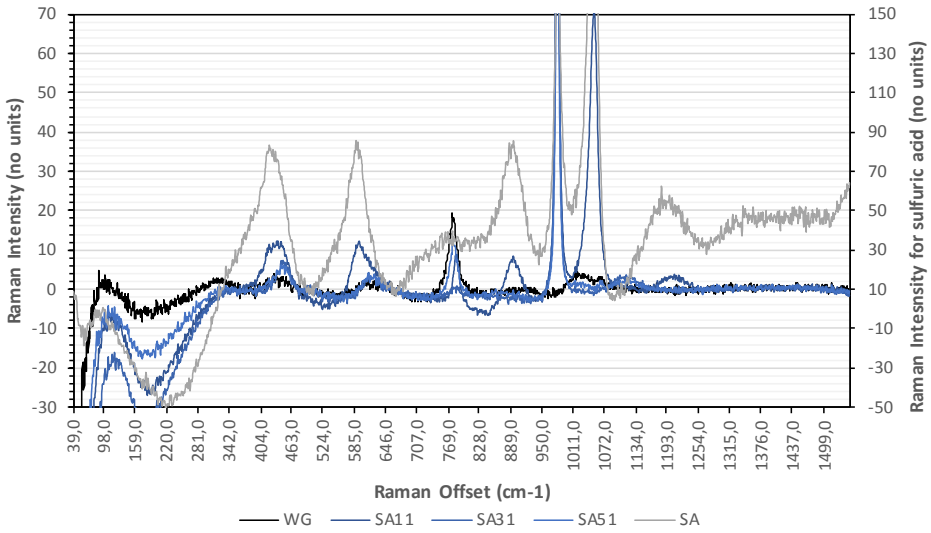

Fig. 16. Raman spectra of sulfuric acid related solutions

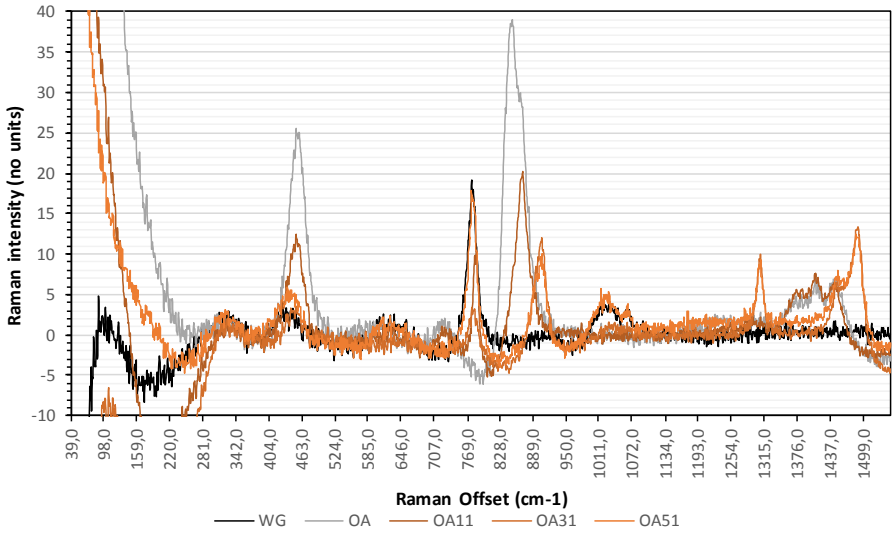

Fig. 17. Raman spectra of oxalic acid related solutions

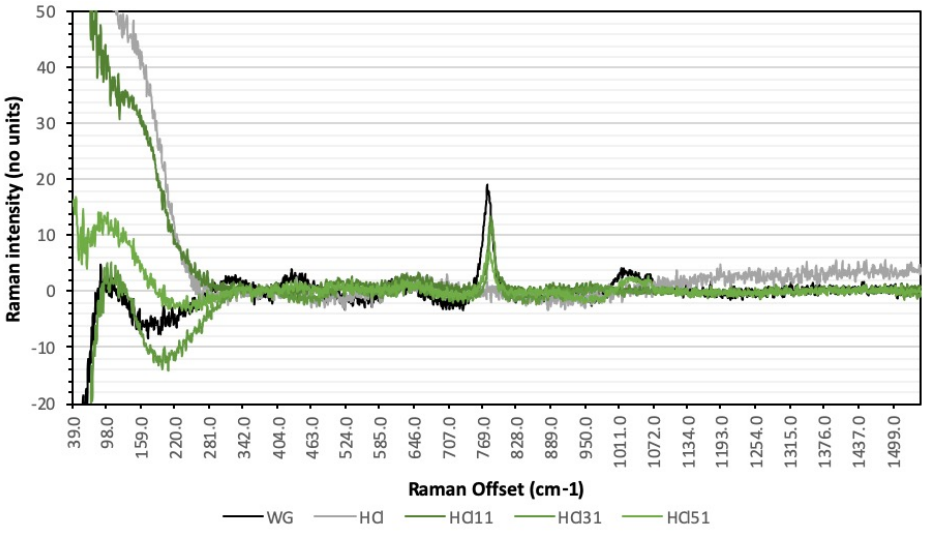

Fig. 18. Raman spectra of hydrochloric acid related solutions

References

ATADEMIR, M.R., KITCHENER, J.A., SHERGOLD, H.L., 1980. *The surface chemistry and flotation of scheelite, II. Flotation "collectors"*. International Journal of Mineral Processing 80, 8(1), 9-16.

AZIZI, D., LARACHI, F., 2018. *Surface interactions and flotation behavior of calcite, dolomite and ankerite with alkyl hydroxamic acid bearing collector and sodium silicate*. Colloids and Surfaces A: Physicochemical and Engineering Aspects 537, 126-138.

BALINSKI, A., 2019. *Grundlagenuntersuchungen zur Aufschließbarkeit von Eudialyt und der sich anschließenden Abtrennung der Seltenerd-Gruppe*. Fakultät für Werkstoffwissenschaft und Werkstofftechnologie, Technische Universität Bergakademie Freiberg, Freiberg, Germany, p. 139.

BELTON, D.J., DESCHAUME, O., PERRY, C.C., 2012. *An overview of the fundamentals of the chemistry of silica with relevance to biosilicification and technological advances*. FEBS J 279(10), 1710-1720.

BERLINSKII, A.I., KLYUEVA, N.D., 1972. *Interaction of alkaline and acidic water glass with some calcium minerals studied by infrared spectroscopic method*. Obogashchenie Rud 17, 16-18.

BULATOVIC, S., 2007. *Handbook of Flotation Reagents: Chemistry, Theory and Practice and Flotation of Sulfide Ores*. 1st Edition, Elsevier.

CASAS, J.M., ALVAREZ, F., CIFUENTES, L., 2000. *Aqueous speciation of sulfuric acid–cupric sulfate solutions*. Chemical Engineering Science 55(24), 6223-6234.

CASTRO, S., MIRANDA, C., TOLEDO, P., LASKOWSKI, J.S., 2013. *Effect of frothers on bubble coalescence and foaming in electrolyte solutions and seawater*. International Journal of Mineral Processing 124, 8-14.

CORDES, P., 2006. *Streng biomimetische Modellsysteme für die Biomineralisation von Siliciumdioxid auf der Basis von Polyaminen oder Alkylglycosiden*. Naturwissenschafltiche Fakultät, Universität Hannover, Hannover, Germany, p. 175.

COX, R.A., HALDNA, U.L., IDLER, K.L., YATES, K., 1981. *Resolution of Raman spectra of aqueous sulfuric acid mixtures using principal factor analysis*. Canadian Journal of Chemistry 59(17): 2591-2598.

CRAIG, V.S.J., 2004. *Bubble coalescence and specific-ion effects*. Current Opinion in Colloid & Interface Science 9(1), 178-184.

DENG, J., LIU, C., YANG, S., LI, H., LIU, Y., 2019. *Flotation separation of barite from calcite using acidified water glass as the depressant*. Colloids and Surfaces A: Physicochemical and Engineering Aspects 579, 123605.

DENG, R., YANG, X., HU, Y., KU, J., ZUO, W., MA, Y., 2018. *Effect of Fe(II) as assistant depressant on flotation separation of scheelite from calcite*. Minerals Engineering 118, 133-140.

DONG, L., JIAO, F., QIN, W., ZHU, H., JIA, W., 2018. *Effect of acidified water glass on the flotation separation of scheelite from calcite using mixed cationic/anionic collectors*. Applied Surface Science 444, 747-756.

FANDRICH, R., GU, Y., BURROWS, D., MOELLER, K., 2007. *Modern SEM-based mineral liberation analysis*. International Journal of Mineral Processing 84(1–4), 310-320.

FENG, B., LUO, X., WANG, J., WANG, P., 2015. *The flotation separation of scheelite from calcite using acidified sodium silicate as depressant*. Minerals Engineering 80, 45-49.

FOUCAUD, Y., FILIPPOVA, I.V., FILIPPOV, L.O., 2019a. *Investigation of the depressants involved in the selective flotation of scheelite from apatite, fluorite, and calcium silicates: Focus on the sodium silicate/sodium carbonate system*. Powder Technology 352, 501-512.

FOUCAUD, Y., BADAWI, M., FILIPPOV, L.O., BARRES, O., FILIPPOVA, I.V., LEBEGUE, S., 2019b. *Synergistic adsorptions of Na2CO3 and Na2SiO3 on calcium minerals revealed by spectroscopic and ab initio molecular dynamics studies*. Chemical Science Journal 10(43), 9928-9940.

FOUCAUD, Y., LEBÈGUE, S., FILIPPOV, L.O., FILIPPOVA, I.V., BADAWI, M., 2018. *Molecular Insight into Fatty Acid Adsorption on Bare and Hydrated (111) Fluorite Surface*. The Journal of Physical Chemistry B 122(51), 12403-12410.

FUERSTENAU, M., GUTIERREZ, G., ELGILLANI, D.A., 1968. *The influence of sodium silicate in nonmetallic flotation systems*. Transactions AIME, New York, 319-323.

GAO, Y., GAO, Z., SUN, W., HU, Y., 2016. *Selective flotation of scheelite from calcite: A novel reagent scheme*. International Journal of Mineral Processing, 154, 10-15.

HALASZ, I., AGARWAL, M., LI, R., MILLER, N., 2007. *Vibrational spectra and dissociation of aqueous Na2SiO3 solutions*. Catalysis Letters 117(1), 34-42.

HEINIG, T., BACHMANN, K., TOLOSANA-DELGADO, R., VAN DEN BOOGAART, K.G., GUTZMER, J., 2015. *Monitoring gravitational and particle shape settling effects on MLA sample preparation*. IAMG Conference 2015, Freiberg, Germany.

HOANG, D.H., HEITKAM, S., KUPKA, N., HASSANZADEH, A., PEUKER, U.A., RUDOLPH, M., 2018. *Froth properties and entrainment in lab-scale flotation: A case of carbonaceous sedimentary phosphate ore*. Chemical Engineering Research and Design 142, 100-110.

HOANG, D., SAQURAN, S., HASSANZADEH, A., KUPKA, N., MICHAUX, B., SCHACH, E., SPRENGER, H., RUDOLPH, M., 2019. *Impact of milling condition on the flotation of Vietnamese silicaceous carbonaceous apatite ore*, IMPC Eurasia 2019. Antalya, Turkey, Turkish Mining Development Foundation, 841-852.

ILER, R.K., 1979. *The Chemistry of Silica: Solubility, Polymerizationm Colloid and Surface Properties and Biochemistry*. John Wiley & Sons, USA.

KINDERMANN, G., 2019. *R get and restrain number of local maxima position and value*. Stackoverflow.

KUPKA, N., MÖCKEL, R., RUDOLPH, M., 2020a. *Acidified water glass in the selective flotation of scheelite from calcite, Part I: performance and impact of the acid type*. Physicochemical Problems of Mineral Processing 56(2), 238-251.

KUPKA, N., RUDOLPH, M., 2018, *Role of sodium carbonate in scheelite flotation – A multi-faceted reagent.* Minerals Engineering 129, 120-128.

KUPKA, N., TOLOSANA-DELGADO, R., SCHACH, E., BACHMANN, K., HEINIG, T., RUDOLPH, M., 2020b. *R as an environment for data mining of process mineralogy data: A case study of an industrial rougher flotation bank*. Minerals Engineering 146, 106111.

LIU, C., FENG, Q., ZHANG, G., CHEN, W., CHEN, Y., 2016, *Effect of depressants in the selective flotation of scheelite and calcite using oxidized paraffin soap as collector*. International Journal of Mineral Processing 157, 210-215.

LIU, X., HUANG, G.-Y., LI, C.-X., CHENG, R.-J., 2015. *Depressive effect of oxalic acid on titanaugite during ilmenite flotation*. Minerals Engineering 79, 62-67.

LUNEVICH, L., 2019. *Aqueous Silica and Silica Polymerisation, In Desalination - Challenges and Opportunities*. IntechOpen, Online.

MARINAKIS, K.I., SHERGOLD, H.L., 1985. *Influence of sodium silicate addition on the adsorption of oleic acid by fluorite, calcite and barite*. International Journal of Mineral Processing 14(3), 177-193.

MARTINS, J.I., AMARANTE, M.M., 2012. *Scheelite Flotation From Tarouca Mine Ores*. Mineral Processing and Extractive Metallurgy Review 34(6), 367-386.

MICHAUX, B., RUDOLPH, M., REUTER, M., 2018. *Challenges in predicting the role of water chemistry in flotation through simulation with an emphasis on the influence of electrolytes*. Minerals Engineering 125, 252-264.

MISHRA, S.K., 1982. *Electrokinetic properties and flotation behaviour of apatite and calcite in the presence of sodium oleate and sodium metasilicate*. International Journal of Mineral Processing 9(1), 59-73.

NEETHLING, S.J., BRITO-PARADA, P.R., 2018. *Predicting flotation behaviour – The interaction between froth stability and performance*. Minerals Engineering 120, 60-65.

PATIL, D., NAYAK, U., 1985. *Selective Flotation of Scheelite and Calcite*.

RAO, K.H., FORSSBERG, K.S.E., 1991. *Mechanism of oleate interaction on salt-type minerals Part III. Adsorption, zeta potential and diffuse reflectance FT-IR studies of scheelite in the presence of sodium oleate*. Colloids and Surfaces 54, 161-187.

SAKSENA, B. D., 1940. *Raman Spectra of some esters of di-carboxylic acids*. Proceedings of the Indian Academy of Sciences - Section A 12(4): 416.

SCHACH, E., LEISTNER, T., RUDOLPH, M., 2017. *The smaller the valuables, the poorer the recovery - Is that always true?* Flotation '17, ed. MEI, Cape Town, South Africa.

SCHACH, E., BUCHMANN, M., TOLOSANA-DELGADO, R.,, LEIßNER, T., KERN, M., VAN DEN BOOGAART, K.G., RUDOLPH, M., PEUKER, U.A., 2019. *Multidimensional characterization of separation processes – Part 1: Introducing kernel methods and entropy in the context of mineral processing using SEM-based image analysis*, Minerals Engineering 137, 78-86.

SJÖBERG, S., 1996. *Silica in aqueous environments*. Journal of Non-Crystalline Solids 196, 51-57.

SPINDE, K., 2012. *Molekulare Mechanismen der Wechselwirkung von Kieselsäure mit organischen Templaten bei der biologichen/biomimetischen Silikatbildung*, Fakultät Mathematik und Naturwissenschaften, Technischen Universität Dresden, Dresden, 109.

SUTHERLAND, K.L., 1948. *Physical chemistry of flotation. XI: Kinetics of the flotation process*, Journal of Physical and Colloid Chemistry 52(2), 394-425.

TIAN, J., XU, L., SUN, W., ZENG, X., FANG, S., HAN, H., HONG, K., HU, Y., 2019. *Use of Al2(SO4)3 and acidified water glass as mixture depressants in flotation separation of fluorite from calcite and celestite*. Minerals Engineering 137, 160-170.

VIDAL, L., JOUSSEIN, E., COLAS, M., CORNETTE, J., SANZ, J., SOBRADOS, I., GELET, J.L., ABSI, J., ROSSIGNOL, S., 2016. *Controlling the reactivity of silicate solutions: A FTIR, Raman and NMR study*. Colloids and Surfaces A: Physicochemical and Engineering Aspects 503, 101-109.

WERES, O., YEE, A., TSAO, L., 1980. *Kinetics of Silica Polymerization*. Report LBL-7033. Earth Sciences Division, Lawrence Berkeley Laboratory, University of California.

WILHELM, S., KIND, M., 2015. *Influence of pH, Temperature and Sample Size on Natural and Enforced Syneresis of Precipitated Silica*. Polymers 7(12), 2504-2521.

YANG, X., ROONASI, P., HOLMGREN, A., 2008. *A study of sodium silicate in aqueous solution and sorbed by synthetic magnetite using in situ ATR-FTIR spectroscopy*. Journal of Colloid and Interface Science 328(1), 41-47.

YANG, Y., XU, L., TIAN, J., LIU, Y., HAN, Y., 2016. *Selective flotation of ilmenite from olivine using the acidified water glass as depressant*. International Journal of Mineral Processing 157, 73-79.

YIANATOS, J., CONTRERAS, F., 2010. *Particle entrainment model for industrial flotation cells*. Powder Technology 197(3), 260-267.

YIN, W.Z., WANG, J.Z., SUN, Z.M., 2015. *Structure–activity relationship and mechanisms of reagents used in scheelite flotation*. Rare Metals 34(12), 882-887.

YONGXIN, L., CHANGGEN, L., 1983. *Selective flotation of scheelite from calcium minerals with sodium oleate as a collector and phosphates as modifiers. I. Selective flotation of scheelite*. International Journal of Mineral Processing 10(3), 205-218.

ZHOU, Q., LU, S., 1992. *Acidized sodium silicate - an effective modifier in fluorite flotation*. Minerals Engineering 5(3), 435-444.

ZHUL, R.W., AMJAD, Z., 2013. *Solution chemistry impact on silica polymerization by inhibitors*. In Mineral Scales in Biological and Industrial Systems, 1st Edition. CRC Press: 174-200.